Hydrol. Earth Syst. Sci. Discuss., https://doi.org/10.5194/hess-2017-407
Manuscript under review for journal Hydrol. Earth Syst. Sci.
Discussion started: 11 September 2017

Hydrology and Earth System Sciences
Open Access
EGU
Discussions

High-resolution ensemble projections and uncertainty assessment of regional climate change over China in CORDEX East Asia

Huanghe Gu[1,2], Zhongbo Yu[1,2], Chuanguo Yang[1,2], Qin Ju[1,2], Tao Yang[1,2]

[1] State Key Laboratory of Hydrology-Water Resources and Hydraulic Engineering, Hohai University, Nanjing, China
[2] College of Hydrology and Water Resources, Hohai University, Nanjing, China

Correspondence to: Zhongbo Yu (zyu@hhu.edu.cn, tel: 086-13675185482)

Abstract. An ensemble simulation of 5 regional climate models (RCMs) from the Coordinated Regional Downscaling Experiment in East Asia (CORDEX-East Asia) was evaluated and used for future regional climate change projection in China. Meanwhile, the contributions of model uncertainty and internal variability are identified. The RCMs simulated both the historical climate (1989-2008) and future climate projection (2030-2049) under the Representative Concentration Pathway (RCP) RCP4.5 scenario. We highlighted 5 subregions in China, viz. Northeast China, North China, South China, Northwest China, and Tibetan Plateau. Our results showed that the capability of RCMs to capture the climatology, annual cycle and inter-annual variability of temperature and precipitation and multi-model ensemble outperforms the individual RCM. For the future climate, consistent warming trends around 1 ℃ were indicated by multi-model ensemble over the whole domain and more pronounced warming was projected in northern and western China. The annual precipitation is likely to increase in most of the simulation region, except the Tibetan Plateau which decreases -7.8%. Compare with the similar seasonal temperature changes with the driving global climate model (GCM), the seasonal precipitation change shows significant inter-RCM difference and has larger magnitude and variability than driving GCM. The model uncertainty for future temperature projection is clearly dominant over the northeast, northwest China and Tibetan Plateau, reaching up to 70%, and it contribute about 40% of the total uncertainty over north and south China. For precipitation, the internal variability is dominant over most regions except for the Tibetan Plateau which the model uncertainties reach up to 60%. In addition, the model uncertainty increases with prediction lead time over all subregions.

1 Introduction

The globally averaged surface temperature has increased by 0.65-1.06 ℃ during the period from 1880 to 2012 according to multiple independently produced datasets, and further rises on the order of 0.3-4.8 ℃ are projected for 2081-2100 relative to 1986-2005 using a set of global climate models (GCMs) driven by the Representative Concentration Pathway (RCP) scenarios RCP2.6 to RCP8.5 (IPCC, 2013). Meanwhile, other climate factors are also changing such as precipitation amounts and variability, snow and ice cover patterns and mean sea level (Alfieri *et al*., 2015; Kerr, 2008; Patz *et al*., 2005). Reliable regional future climate projection is important for the evaluation of climate change impacts and vulnerability, as

well as the elaboration of appropriate mitigation and adaptation measures, especially for the developing countries like China tend to be one of the most vulnerable to the adverse effects of climate changes.

The East Asian summer monsoon (EASM) is the most distinctive climate feature in China, and the monsoon area accounts for approximately 60% of mainland (Ding and Chan, 2005). EASM system-related precipitation starts around mid-May or even earlier in Indo-China Peninsula, presents distinct stepwise northward and northeastward advances feature with two abrupt northward jumps and three stationary periods, and begins withdrawing southward in September (Ding, 2004; Hsu, 2005). The rainy seasons of EASM, including the pre-summer rainy season over South China, mei-yu (in China) occur normally during the stationary periods which are imbedded in the northward advance of the summer monsoon. The anomaly of EASM could cause floods and droughts which plays a crucial role in the livelihood of more than one billion people (Webster *et al*., 1998). However, because of the complex topography and model limitation, how to reliably reproduce the climatological rainfall and interannual variation of EASM still remains a challenge. The CMIP3 (coupled model intercomparison project phase 3) and CMIP5 GCMs, however, have problems simulating precipitation in this region. Recent studies have suggested that the new generation of GCMs from CMIP5 archive shows some improvements to reproduce the climatology and interannual variability of EASM compared with the CMIP3 GCMs, but the simulated biases remained and large intermodel spread existed (Chen and Bordoni, 2014; Gu *et al*., 2015; Huang *et al*., 2013; Song and Zhou, 2013). For example, the mei-yu rainfall band is missing in the GCMs, although the monsoon circulation is well reproduced (Ding and Chan, 2005; Song and Zhou, 2013).

Because of these deficiencies, higher resolution GCMs have been developed to improve the capabilities in monsoon features simulation including orographic precipitation, low-level jet orientation and variability, as well as the mei-yu onset and withdrawal (Kitoh and Kusunoki, 2008; Kitoh *et al*., 2013; Kusunoki *et al*., 2006). However, these experiments are still burdensome due to large computation resources required for multi-decadal simulations. Therefore the regional climate models (RCMs) forces on a region of interest are commonly used in regional climate projection and climate change impacts studies (Christensen *et al*., 2007; Gallée *et al*., 2004; Gao *et al*., 2006; Giorgi and Mearns, 1999; Gu *et al*., 2012; Leung *et al*., 2003; Wang *et al*., 2004; Yira *et al*., 2017; Yu *et al*,. 2006). The ongoing coordinated regional downscaling experiment (CORDEX) (Giorgi *et al*., 2009; Jones *et al*., 2011), whose aim to provide high-resolution regional future climate projections for the majority of populated land regions on the globe by using multi-RCMs, and an interface to the applicants of the climate simulations in climate change impact, adaptation, and mitigation studies. The CORDEX-EA is the East-Asian branch of the CORDEX experiment and provides ensemble regional climate simulations (https://cordex-ea.climate.go.kr/main/modelsPage.do). The CORDEX-EA has been evaluated for simulating the precipitation and temperature over East Asia (Huang *et al*., 2015; Jin *et al*., 2016; Lee and Hong, 2014; Oh *et al*., 2013; Park *et al*., 2013; Suh *et al*., 2012; Zou *et al*., 2014).

Despite large improvements in the simulating of local processes, future climate projections are still accompanied by large uncertainties stemming from different sources, including the forcing GCMs, emission scenarios, downscaling methods (RCMs or statistical downscaling methods), and natural climate internal variability (Déqué *et al*., 2007; Deser *et al*., 2012).

Numerous previous studies have demonstrated that GCMs being the main source of uncertainty (Seo *et al*., 2016). However, after excluding the outliers from the GCM ensemble, other uncertainty sources like RCMs and internal variability will became more important than GCMs (Kay *et al*., 2009; Wilby and Harris, 2006). In a non-stationary climate, the internal variability of a given GCM-RCM chain can remain high above the trend related to a given emission scenarios forcing (Deser *et al*., 2012; Hawkins and Sutton, 2011; Lafaysse *et al*., 2014; O'Brien *et al*., 2011). So far, little attention has been paid to quantify the contributions of the uncertainty arising from RCMs and internal variability in future climate projection over China. Thus, it is necessary to objectively evaluate the capability of RCMs and quantify the uncertainty in future climate projections.

In this study, we evaluate the performance of five RCMs within CORDEX-EA to reproduce present-day climate and to analyze the projected future climate changes under the middle emission scenario. In addition, biases in current climate simulations and uncertainties in future climate projections attributed to the RCMs and internal variability are further analyzed. This paper is structured as follows. The data from observation and model simulation, and analysis method are described in next section. Scection 3 presents the historical performances of RCMs for temperature and precipitation and future climate changes under RCP4.5 emission scenario over China. The uncertainties in regional future climate projection resulting from inter-RCMs and natural climate internal variability are also discussed. The summary and conclusion are given in section 4.

2 Data and methods

2.1 Observations

The reference temperature and precipitation data used to compare the model results to observation data develops from the University of East Anglia Climate Research Unit Timeseries 3.23 (CRU TS3.23), with a spatial resolution 0.5 °, derived from gauge measurements, details in Harris et al., (2014). The Asian Precipitation-Highly Resolved Observational Data Integration Toward Evaluation (APHRODITE) dataset with a spatial resolution 0.25 ° also was used for RCMs evaluation (Yatagai et al., 2012). In order to facilitate comparison, outputs from a host of RCMs were converted to a common grid of 0.5 °×0.5 ° latitude/longitude as in the remapped to the CRU and APHRO observations, using bilinear interpolation. The use of two data sets is beneficial not only to the evaluation of RCM's performance but also to the verification of the observation datasets.

2.2 Models and experiments

In this study, we used five RCMs, namely, HadGEM3-RA, MM5, WRF, RegCM4, and RSM for East Asian climate experiments (Table 1). The dataset were produced from multi-RCM national project under Korea Meteorological Administration. The spatial resolution of the data is 50 km (except HadGEM3-RA is 0.44 °), and the whole CORDEX-EA domain includes East Asia, India, the Western Pacific Ocean, and the northern part of Australia, as shown in Fig. 1. Model

configurations include physical schemes are summarized in Table 1. The detailed description of each of the RCM simulations can be found in Suh et al. (2012) and Park et al. (2016).

Table 1

Figure 1

In this study, two types of current climate experiments from five RCMs were performed, including the evaluation (hereafter EVAL) experiment for the period of 1989-2007 and historical (HIST) experiment for the period of 1980-2005. The EVAL experiment acquires initial and boundary conditions from the National Centers for Environmental Prediction (NCEP) reanalysis and the HIST experiment is forced by the Atmosphere-Ocean coupled Hadley Center Global Environmental Model version 2 (HadGEM2-AO) simulation. The HadGEM2-AO (1.875 °×1.25 ° horizontal resolution) has been used for climate simulations in a CMIP5 set of long-term experiments, and has been evaluated to have a reasonable ability to capture the East Asian climatology (Baek *et al*., 2013; Martin *et al*., 2011; Sperber *et al*., 2013). The future climate simulation is driven from the HadGEM2-AO under RCP 4.5 scenario. The RCP 4.5 scenario is an intermediate scenario and a cost-minimizing pathway that total radiative forcing is stabilized at 4.5 W m^{-2} in the year 2100 (Thomson *et al*., 2011). The reference period from 1980 to 1999 and the scenario period from 2030 to 2049 are analyzed for climate changes study.

The multi-model ensemble (MME) mean, which is defined as the pointwise arithmetic average over all individual model climatologies, is used to narrow down inter-RCM uncertainties because of their differences in model structures and physics. To further evaluate the model performance on smaller spatial scales, we evaluate the performance of RCMs over five selected sub-regions, that is, Northeast China (40-50 ℃N, 115-130 ℃E), North China (30-40 ℃N, 105-120 ℃E), South China (22-30 ℃N, 105-120 ℃E), Northwest China (35-45 ℃N, 80-95 ℃E), and Tibetan Plateau (28-35 ℃N, 80-95 ℃E).

2.3 Analysis methods

We evaluate climatology from individual RCMs, MME using bias, the root-mean-square error (RMSE), and Taylor diagram analysis. The annual and seasonal means are examined by bias and RMSE. The model performance on spatial patterns is evaluated by Taylor diagram (Taylor, 2001).

In this study, all RCMs are driven by the same GCM under the same scenario, so the uncertainty of the climate projections is mainly caused by the inter-RCM variability and internal variability (Niu *et al*., 2015). The method developed by Hawkins and Sutton (2009; 2011) was used for separating these two sources of uncertainty.

The raw simulation of each model $X_{m,t}$ for the model m and year t which can be expressed by

$$X_{m,t} = x_{m,t} + c_m + \varepsilon_{m,t} \quad (1)$$

where the smooth fit is represented by $x_{m,t}$, the reference data is denoted by c_m, and the residual is denoted by $\varepsilon_{m,t}$. Here each individual simulation was fit with a fourth-order polynomial by using ordinary least squares method during the years 2030-2049. The reference data used are the mean of the years 1980 to 1999 and estimated from the smooth fits.

Hydrol. Earth Syst. Sci. Discuss., https://doi.org/10.5194/hess-2017-407
Manuscript under review for journal Hydrol. Earth Syst. Sci.
Discussion started: 11 September 2017

Hydrology and Earth System Sciences
Open Access
EGU
Discussions

The RCMs are weighted by their performance in simulating the current climate from the mean of 1980-1999, up to the year 1999. Thus, each model is weighted according to

$$w_m = \frac{1}{x_{obs} + \left| x_{m,1999} - x_{obs} \right|} \quad (2)$$

where $x_{m,1999}$ is the model climate changes at the year of 1999, relative to 1980-1999, and x_{obs} is an observational estimate derived from fitting a similar fourth-order polynomial to the observations. The normalized quantities of these weightings can be expressed as

$$W_m = \frac{w_m}{\sum_m w_m} \quad (3)$$

The internal variability (equ. 4) is defined as the multi-model mean of theses variance of the residuals from the fits for each model,

$$V = \sum_m W_m \, \mathrm{var}_t(\varepsilon_m, t) \quad (4)$$

$$M(t) = \mathrm{var}_m(x_{m,t}) \quad (5)$$

And the intermodel variability (equ.5) is estimated from the variance in the different RCM prediction fits ($x_{m,t}$), where $\mathrm{var}_t(.)$ and $\mathrm{var}_m(.)$ indicate the variance across time and model, respectively.

It was assumed that the two sources of uncertainty can be treated independently (i.e., there is no interaction between them). Thus, the total variability V_T is then

$$V_T(t) = V + M(t) \quad (6)$$

3 Results

3.1 Climatology for the control climate

Figure 2 shows annual average temperature of CRU and multi-model ensemble, and the temperature biases of five RCMs driving by HadGEM2-AO during 1980 to 2005. The corresponding MME mean is denoted by point ensemble. Similar as the multi-model average results, all RCMs could reproduce the spatial pattern which demonstrates a decreasing south-north gradient of the observed temperature over China and a cold area over the Tibetan Plateau. Generally, all models give warm biases over most domain, especially MM5 and HadGEM3-RA give larger warm biases than the other models. Most RCMs give obvious warm biases over the Tibetan Plateau except for RSM which give a cold biases. The multi-model ensemble shows overall best results to reproduce the temperature spatial distribution and give less than 1 ℃ temperature biases over most area of China.

Figure 2

The RCMs give reasonably accurate simulations on temperature, but are less successful at reproducing the precipitation. Figure 3 shows annual average precipitation of CRU, APHRO, multi-model ensemble, and the precipitation biases of five RCMs in current period. Observed precipitation amounts also show a spatial pattern with decreasing southeast-northwest gradient over China. All RCMs successfully simulate the precipitation patterns but with quite large biases in amounts. The precipitation is overestimated in the arid/semiarid region of northwest China by all RCMs except for WRF which underestimate the precipitation over the whole domain. Comparably, RegCM shows more realistic in current precipitation reproduction. In general, the multi-model ensemble outperforms the individual RCM in reproducing the observed spatial pattern of precipitation.

Figure 3

The comparison of the spatial variability statistics of the models in reproducing the annual mean temperature and precipitation by the Taylor plot (Taylor, 2001) are summarized in Figure 4. The temperature simulation from five RCMs display a good spatial pattern correlation range from 0.83 to 0.96, while the precipitation simulation show a relatively wide range of spatial pattern correlations from 0.29 to 0.93. It should be noted that the RMSE of the ensemble statistic is less than most of single model simulation. In other words, the apparent biases of the individual models are reduced by the multi-model ensembles.

There could be several reasons for this phenomenon, which also noticed by other scholars in their model inter-comparisons (Phillips and Gleckler, 2006). First, to a certain extent that the bias of a simulated climate field is symptomatic of random error, and the multi-model ensemble may reduce or counteract this error. Moreover, the pointwise variations of climate field have been smooth out by averaging, thereby filtering regional scale simulations, where current climate models are difficult to capture. However, their causes are often difficulty to identify and to remedy, further investigation is needed in model inter-comparison. In addition, most of RCMs show better performance than the driving GCM HadGEM2-AO, and it reflect the added value of the high resolution RCMs in simulation of spatial variability of the East Asia monsoon.

Figure 4

The ability of a climate model to capture realistic interannual variability is an important measure of its performance. The time series of the annual mean temperature and precipitation from RCMs are compared to CRU and APHRO in Figure 5. The interannual variation of the climatologies is well reproduced in RCMs ensemble. In the evaluation experiment for 1989-2007, the correlation coefficient of the annual climatologies time series at five subregions between observation and RCMs ensemble is range from 0.52 to 0.78 for temperature, and range from 0.50 to 0.87 for precipitation. The correlation coefficient is lower in West China compare with the East China, especially in Tibetan Plateau. In the historical experiment for 1980-2005, the RCMs have difficulty to reproduce the interannual variability for precipitation because of the impact of the driving GCM.

Figure 5

The temporal distribution of rainfall throughout the year is quite importance for the ecosystems and water resource management. In order to evaluate the RCM's ability to capture the seasonal variability of climatologies, the seasonal cycles of simulated temperature and precipitation averaged over five subregions in China was examined (Figures 6). The observed temperature and precipitation show the steep onset of summer rainfall associated with the summer monsoon, which peaks sharply in July (except south China in June for precipitation). All RCMs successfully reproduce the seasonal variation characteristics of a single peak. All models capture the bell-shape of the monthly temperature profile. But almost all RCMs overestimate the temperature the whole year with systematic biases except for WRF which underestimate the temperature over most regions. Overall, the RCMs show better in simulating the twenty-year average monthly temperature than the corresponding precipitation. The multi-model ensemble succeed in reproducing the seasonal variation of precipitation. However, the inter-model difference is quite larger compare with the temperature. Some RCMs always underestimate (i.e. WRF) or overestimate (i.e. MM5 and HadGEM3-RA) the precipitation especially in summer, other RCM (i.e. RSM) overestimate precipitation in some region/season but underestimate precipitation in others. Overall, RegCM and multi-model ensemble give the most accurate twenty-year average climate simulation.

Figure 6

3.2 Multi-RCM future climate projection

3.2.1 Futrue change in climatology

The projected future changes in annual mean temperature show similar warming trends over the whole domain for the period 2030-2049 under RCP4.5 emission scenario (Fig. 7). All five model project substantially significant warming while exhibits different spatial patterns. The ensemble averaged annual temperature increases are 1.3, 1.0, 0.9, 1.2, and 1.3 ℃ over the Northeast, North, South, Northwest, and Tibetan Plateau subregions, respectively. The warming in northern and western China is more significant than southern China, especially in Northeast China and Tibetan Plateau, which are similar with observation and projection of models (Sun *et al.*, 2014; You *et al.*, 2014; Zhou and Yu, 2006).

Figure 7

Figure 8 shows the spatial distributions of annual precipitation changes (RCP4.5 – baseline). In the future period, 2030-2049, the multi-model averaged precipitation change is positive over China, with all five individual model exhibiting positive changes over all five subregions. The most prominent precipitation increases are shown in MM5, RSM, and RegCM over the north and northwest China. The annual precipitation changes little over central China, northern China and southwestern China. In Tibetan Plateau a decrease in order of -7.8% is projected. There are some broad similarities across RCMs because they have the same parent GCM, but among those, the signal for change is more mixed in WRF.

Figure 8

Table 2

3.2.2 Change in seasonal cycle

The future changes of temperature and precipitation are characteristic of regionality and seasonality. The ensemble projection (as shown in Figure 9) indicates that the monthly temperature change over five subregions in China is in the range from 0.3 ℃ to 2.2 ℃ under RCP4.5 scenario. All RCMs projections show that there is a more remarkable trend to become warm in colder months from November to March than in other months. Most RCMs project positive monthly precipitations changes for summer (from June to August) in northeast, north, and south China. The spreads in monthly precipitation changes by five RCMs are characteristic of seasonality, with largest appearing in July and the smallest in March. Additionally, the seasonal cycle of temperature change in multi-model ensemble is similar to that of the driving GCM HadGEM-AO. However, the seasonal precipitation change in multi-model ensemble has larger magnitude and variability than driving GCM. This phenomenon concerns the significance of the model physics and processes for future climate projection.

Figure 9

3.2.3 Inter-RCM variability of Multi-RCM projections

The uncertainties of regional climate projection are arised from different sources, which include the GCMs, emission scenarios, RCMs, and natural climate internal variability. In this study, the regional future climate is projected by using five RCMs forced with the same GCM under an intermediate scenario (RCP4.5). As a consequence, the contribution of inter-RCM variability and natural climate internal variability to total uncertainty are analyzed in this section.

The contributions to the total prediction uncertainty from model uncertainty and natural climate internal variability were estimated by the method proposed by Hawkins and Sutton (2009), and the results for five subregions were shown in Figure 10. It shows that the relative importance of the model uncertainty increases with prediction lead time over all subregions. For temperature, the model uncertainty is primary source of uncertainty over the northeast, northwest China and Tibetan Plateau during 2030-2049, reaching up to 70%. The model uncertainty contribute smaller (about 40%) of the total uncertainty over north and south China before the middle of the 21st century. For precipitation, the internal variability is dominant over most regions except for the Tibetan Plateau which the model uncertainties reach up to 60%. The uncertainties come from the driving GCM and the emission scenarios are not discussed in this study, although they have been recognized as important component for total uncertainty (Déqué *et al.*, 2012). More robust estimates include larger ensemble of projections by RCMs forced by different GCMs and emission scenarios are necessary for the uncertainty quantification.

Figure 10

4 Summary and conclusions

In this research, simulation of five RCM models run within the CORDEX-EA initiative at 50km resolution with boundary forcing from a CMIP5 global model applying the RCP4.5 scenario are employed to derive the future climate change signal

for the China and five selected smaller investigation areas. In this study, we focus on the future regional climate projection over China and the quantification of model uncertainty and natural climate internal variability.

The control runs of CORDEX-EA RCMs reveal an overall reasonable representation of the mean climate properties when compared with observational gridded dataset. In general, all RCMs give warm biases while the multi-model ensemble shows overall best performance with less than 1 ℃ annual average temperature biases over most area of China. The control RCM results have a significant spread, and show quite large biases in annual precipitation. Similarly, the multi-model ensemble outperforms the individual RCM in reproducing the observed spatial pattern of precipitation. The RCMs also have the ability to capture realistic interannual variability and seasonal variability of the annual mean temperature and precipitation. Based upon the model performance evaluation, our results show that the present set of RCMs from CORDEX-EA can be used to provide useful information on climate projections over East Asia.

For the future climate of 2030-2049, consistent warming trends around 1 ℃ were indicated by multi-model ensemble over the whole domain and more pronounced warming was projected in northern and western China. The spread between the single simulations is in the order of 1.3 ℃. The annual precipitation is likely to increase in most of the simulation region, especially in north and northwest China. The annual precipitation decreases or changes little over northeastern China and south China. In Tibetan Plateau a decrease in order of -7.8% is projected. The seasonal temperature changes more drastically in colder months which are similar to that of the driving GCM. However, the seasonal precipitation show positive changes in summer with significant inter-RCM difference and has larger magnitude and variability than driving GCM. The above results manifest that the internal model variability play an important role in the regional climate change projection.

The contributions of model uncertainty and internal variability are identified in this study. The model uncertainty for future temperature projection is clearly dominant over the northeast, northwest China and Tibetan Plateau during 2030-2049, reaching up to 70%, and it can explain about 40% of the total uncertainty over north and south China. For precipitation, the internal variability is dominant over most regions except for the Tibetan Plateau which the model uncertainties reach up to 60%. In addition, the model uncertainty increases with prediction lead time over all subregions. The simulation results of RCM also influenced by the internal physics and boundary conditions from GCMs as discussed in other's studies (Mariotti *et al.*, 2011; Syed *et al.*, 2012). More reliable future climate information could be provided by coupling GCMs and RCMs through the modifications to model structures and parameters.

Acknowledgments

This work was supported by the National Key R&D Program of China (Grant No. 2016YFC0402706, 2016YFC0402710), the National Natural Science Foundation of China (No. 41501015, 41323001, 51539003, 51421006), the Fundamental Research Funds for the Central Universities (2016B00114). We acknowledge the CORDEX-East Asia Databank, which is responsible for the CORDEX dataset, and we thank the National Institute of Meteorological Research (NIMR), three

universities in the Republic of Korea (Seoul National Univ., Yonsei Univ., Kongju National Univ.) and other cooperative research institutes in East Asia region for producing and making available their model output.

References:

Alfieri, L., Burek, P., Feyen, L. and Forzieri, G., 2015. Global warming increases the frequency of river floods in Europe. HYDROLOGY AND EARTH SYSTEM SCIENCES, 19(5): 2247-2260. DOI: 10.5194/hess-19-2247-2015

Baek, H., Lee, J. and Lee, H. et al., 2013. Climate change in the 21st century simulated by HadGEM2-AO under representative concentration pathways. Asia-Pacific Journal of Atmospheric Sciences, 49(5): 603-618. DOI: 10.1007/s13143-013-0053-7

Cha, D. and Lee, D., 2009. Reduction of systematic errors in regional climate simulations of the summer monsoon over East Asia and the western North Pacific by applying the spectral nudging technique. Journal of Geophysical Research: Atmospheres, 114(D14): D14108. DOI: 10.1029/2008JD011176

Chen, J. and Bordoni, S., 2014. Intermodel spread of East Asian summer monsoon simulations in CMIP5. Geophysical Research Letters, 41(4): 1314-1321. DOI: 10.1002/2013GL058981

Christensen, J.H., Hewitson, B. and Busuioc, A. et al., 2007. Regional Climate Projections. In: S. Solomon et al. (S. Solomon et al.)^(S. Solomon et al.s)|,*Climate Change 2007: The Physical Science Basis. Contribution of Working Group 1 to the Fouth Assessment Report of the Intergovernmental Panel on Climate Change. Cambridge University Press, Cambridge, United Kingdom and New York, NY, USA.

Davies, T., Cullen, M.J.P. and Malcolm, A.J. et al., 2005. A new dynamical core for the Met Office's global and regional modelling of the atmosphere. Quarterly Journal of the Royal Meteorological Society, 131(608): 1759-1782. DOI: 10.1256/qj.04.101

Déqué, M., Rowell, D.P. and Luthi, D. et al., 2007. An intercomparison of regional climate simulations for Europe: assessing uncertainties in model projections. Climatic Change, 81(1): 53-70. DOI: 10.1007/s10584-006-9228-x

Déqué, M., Somot, S. and Sanchez-Gomez, E. et al., 2012. The spread amongst ENSEMBLES regional scenarios: regional climate models, driving general circulation models and interannual variability. Climate Dynamics, 38(5): 951-964. DOI: 10.1007/s00382-011-1053-x

Deser, C., Phillips, A., Bourdette, V. and Teng, H., 2012. Uncertainty in climate change projections: the role of internal variability. Climate Dynamics, 38(3-4): 527-546. DOI: 10.1007/s00382-010-0977-x

Ding, Y., 2004. Seasonal march of the East-Asian summer monsoon. In: C.P. Chang (C.P. Chang)^(C.P. Changs)|,*East Asian Monsoon. Mainland Press, Singapore, pp. 3-53.

Ding, Y. and Chan, J.C.L., 2005. The East Asian summer monsoon: an overview. Meteorology and Atmospheric Physics, 89(1): 117-142. DOI: 10.1007/s00703-005-0125-z

Gallée, H., Moufouma-Okia, W. and Bechtold, P. et al., 2004. A high-resolution simulation of a West African rainy season using a regional climate model. Journal of Geophysical Research: Atmospheres, 109(D5): D05108. DOI: 10.1029/2003JD004020

Gao, X.J., Pal, J.S. and Giorgi, F., 2006. Projected changes in mean and extreme precipitation over the Mediterranean region from a high resolution double nested RCM simulation. Geophysical Research Letters, 33: L03706. DOI: 10.1029/2005GL024954

Giorgi, F. and Mearns, L.O., 1999. Introduction to special section: Regional climate modeling revisited. J Geophys Res, 104(D6): 6335-6352. DOI: 10.1029/98JD02072

Giorgi, F., Coppola, E. and Solmon, F. et al., 2012. RegCM4: model description and preliminary tests over multiple CORDEX domains. Climate Research, 52: 7-29. DOI: 10.3354/cr01018

Giorgi, F., Jones, C. and Asrar, G.R., 2009. Addressing climate information needs at the regional level: the CORDEX framework. WMO Bulletin, 58(3): 175-183. DOI:

Gu, H., Wang, G., Yu, Z. and Mei, R., 2012. Assessing future climate changes and extreme indicators in east and south Asia using the RegCM4 regional climate model. Climatic Change, 114(2): 301-317. DOI: 10.1007/s10584-012-0411-y

Gu, H., Yu, Z. and Wang, J. et al., 2015. Assessing CMIP5 general circulation model simulations of precipitation and

temperature over China. International Journal of Climatology, 35(9): 2431 – 2440. DOI: 10.1002/joc.4152

Harris, I., Jones, P.D., Osborn, T.J. and Lister, D.H., 2014. Updated high-resolution grids of monthly climatic observations – the CRU TS3.10 Dataset. International Journal of Climatology, 34(3): 623-642. DOI: 10.1002/joc.3711

Hawkins, E. and Sutton, R., 2009. The Potential to Narrow Uncertainty in Regional Climate Predictions. Bulletin of the American Meteorological Society, 90(8): 1095-1107. DOI: 10.1175/2009BAMS2607.1

Hawkins, E. and Sutton, R., 2011. The potential to narrow uncertainty in projections of regional precipitation change. Climate Dynamics, 37(1-2): 407-418. DOI: 10.1007/s00382-010-0810-6

Hong, S., Park, H. and Cheong, H. et al., 2013. The Global/Regional Integrated Model system (GRIMs). Asia-Pacific Journal of Atmospheric Sciences, 49(2): 219-243. DOI: 10.1007/s13143-013-0023-0

Hsu, H., 2005. East Asian monsoon. In: K.M.L. William and D.E. Waliser (K.M.L. William and D.E. Waliser)^(K.M.L. William and D.E. Walisers)|,*Intraseasonal Variability in the Atmosphere-Ocean Climate System, Berlin, Heidelberg, pp. 63-94.

Huang, B., Polanski, S. and Cubasch, U., 2015. Assessment of precipitation climatology in an ensemble of CORDEX-East Asia regional climate simulations. Climate Research, 64(2): 141-158. DOI: 10.3354/cr01302

Huang, D., Zhu, J., Zhang, Y. and Huang, A., 2013. Uncertainties on the simulated summer precipitation over Eastern China from the CMIP5 models. Journal of Geophysical Research: Atmospheres, 118(16): 9035-9047. DOI: 10.1002/jgrd.50695

IPCC, 2013. Climate Change 2013: the physical basis. Contribution of Working Group 1 to the Fifth Assessment Report of the IPCC. Cambridge University Press, New York.

Jin, C., Cha, D. and Lee, D. et al., 2016. Evaluation of climatological tropical cyclone activity over the western North Pacific in the CORDEX-East Asia multi-RCM simulations. Climate Dynamics, 47(3): 765-778. DOI: 10.1007/s00382-015-2869-6

Jones, C., Giorgi, F. and Asrar, G., 2011. The Coordinated Regional Downscaling Experiment: CORDEX – an international downscaling link to CMIP5. CLIVAR exchanges, 56(16): 34-40. DOI:

Kay, A.L., Davies, H.N., Bell, V.A. and Jones, R.G., 2009. Comparison of uncertainty sources for climate change impacts: flood frequency in England. Climatic Change, 92(1-2): 41-63. DOI: 10.1007/s10584-008-9471-4

Kerr, R., 2008. Global warming-Climate change hot spots mapped across the United States. Science, 321(5891): 909. DOI: 10.1126/science.321.5891.909

Kitoh, A. and Kusunoki, S., 2008. East Asian summer monsoon simulation by a 20-km mesh AGCM. Climate Dynamics, 31(4): 389-401. DOI: 10.1007/s00382-007-0285-2

Kitoh, A., Endo, H. and Krishna Kumar, K. et al., 2013. Monsoons in a changing world: A regional perspective in a global context. Journal of Geophysical Research: Atmospheres, 118(8): 3053-3065. DOI: 10.1002/jgrd.50258

Kusunoki, S., Yoshimura, J. and Yoshimimura, H. et al., 2006. Change of Baiu Rain Band in Global Warming Projection by an Atmospheric General Circulation Model with a 20-km Grid Size. Journal of the Meteorological Society of Japan. Ser. II, 84(4): 581-611. DOI: 10.2151/jmsj.84.581

Lafaysse, M., Hingray, B. and Mezghani, A. et al., 2014. Internal variability and model uncertainty components in future hydrometeorological projections: The Alpine Durance basin. Water Resources Research, 50(4): 3317-3341. DOI: 10.1002/2013WR014897

Lee, J. and Hong, S., 2014. Potential for added value to downscaled climate extremes over Korea by increased resolution of a regional climate model. Theoretical and Applied Climatology, 117(3): 667-677. DOI: 10.1007/s00704-013-1034-6

Leung, L.R., Mearns, L.O., Giorgi, F. and Wilby, R.L., 2003. Regioinal climate research: needs and opportunities. Bulletin of the American Mathematical Society, 84(1): 89-95. DOI: 10.1175/BAMS-84-1-89

Mariotti, L., Coppola, E. and Sylla, M.B. et al., 2011. Regional climate model simulation of projected 21st century climate change over an all-Africa domain: Comparison analysis of nested and driving model results. Journal of Geophysical Research: Atmospheres, 116(D15): D15111. DOI: 10.1029/2010JD015068

Martin, G.M., Bellouin, N. and Collins, W.J. et al., 2011. The HadGEM2 family of Met Office Unified Model climate configurations. Geoscientific Model Development, 4(3): 723--757. DOI: 10.5194/gmd-4-723-2011

Niu, X., Wang, S. and Tang, J. et al., 2015. Multimodel ensemble projection of precipitation in eastern China under A1B emission scenario. Journal of Geophysical Research: Atmospheres, 120(19): 9965-9980. DOI: 10.1002/2015JD023853

O'Brien, T.A., Sloan, L.C. and Snyder, M.A., 2011. Can ensembles of regional climate model simulations improve results

from sensitivity studies? Climate Dynamics, 37(5): 1111-1118. DOI: 10.1007/s00382-010-0900-5

Oh, S., Suh, M. and Cha, D., 2013. Impact of lateral boundary conditions on precipitation and temperature extremes over South Korea in the CORDEX regional climate simulation using RegCM4. Asia-Pacific Journal of Atmospheric Sciences, 49(4): 497-509. DOI: 10.1007/s13143-013-0044-8

Park, C., Min, S. and Lee, D. et al., 2016. Evaluation of multiple regional climate models for summer climate extremes over East Asia. Climate Dynamics, 46(7): 2469 – 2486. DOI: 10.1007/s00382-015-2713-z

Park, J., Oh, S. and Suh, M., 2013. Impacts of boundary conditions on the precipitation simulation of RegCM4 in the CORDEX East Asia domain. Journal of Geophysical Research: Atmospheres, 118(4): 1652-1667. DOI: 10.1002/jgrd.50159

Patz, J.A., Campbell-Lendrum, D., Holloway, T. and Foley, J.A., 2005. Impact of regional climate change on human health. Nature, 438(7066): 310-317. DOI: 10.1038/nature04188

Phillips, T.J. and Gleckler, P.J., 2006. Evaluation of continental precipitation in 20th century climate simulations: The utility of multimodel statistics. Water Resources Research, 42(3): W03202. DOI: 10.1029/2005WR004313

Seo, S.B., Sinha, T. and Mahinthakumar, G. et al., 2016. Identification of dominant source of errors in developing streamflow and groundwater projections under near-term climate change. Journal of Geophysical Research: Atmospheres, 121(13): 7652-7672. DOI: 10.1002/2016JD025138

Skamarock, W.C., Klemp, J.B. and Dudhia, J. et al., 2005. A Description of the Advanced Research WRF Version 2.

Song, F. and Zhou, T., 2013. Interannual Variability of East Asian Summer Monsoon Simulated by CMIP3 and CMIP5 AGCMs: Skill Dependence on Indian Ocean – Western Pacific Anticyclone Teleconnection. Journal of Climate, 27(4): 1679-1697. DOI: 10.1175/JCLI-D-13-00248.1

Sperber, K.R., Annamalai, H. and Kang, I.S. et al., 2013. The Asian summer monsoon: an intercomparison of CMIP5 vs. CMIP3 simulations of the late 20th century. Climate Dynamics, 41(9-10): 2711-2744. DOI: 10.1007/s00382-012-1607-6

Suh, M.S., Oh, S.G. and Lee, D.K. et al., 2012. Development of New Ensemble Methods Based on the Performance Skills of Regional Climate Models over South Korea. Journal of Climate, 25(20): 7067-7082. DOI: 10.1175/JCLI-D-11-00457.1

Sun, Q., Miao, C. and Duan, Q., 2014. Projected changes in temperature and precipitation in ten river basins over China in 21st century. International Journal of Climatology: n/a-n/a. DOI: 10.1002/joc.4043

Syed, F.S., Yoo, J.H., Körnich, H. and Kucharski, F., 2012. Extratropical influences on the inter-annual variability of South-Asian monsoon. Climate Dynamics, 38(7): 1661-1674. DOI: 10.1007/s00382-011-1059-4

Taylor, K.E., 2001. Summarizing multiple aspects of model performance in a single diagram. Journal of Geophysical Research: Atmospheres, 106(D7): 7183-7192. DOI: 10.1029/2000JD900719

Taylor, K.E., 2001. Summarizing multiple aspects of model performance in a single diagram. J Geophys Res, 106(D7): 7183-7192. DOI: 10.1029/2000JD900719

Thomson, A., Calvin, K. and Smith, S. et al., 2011. RCP4.5: a pathway for stabilization of radiative forcing by 2100. Climatic Change, 109(1-2): 77-94. DOI: 10.1007/s10584-011-0151-4

Wang, Y., Leung, L.R. and McGregor, J.L. et al., 2004. Regional climate modeling: progress, challenges, and prospects. Journal of the Meteorological Society Of Japan, 82(6): 1599-1628. DOI: 10.2151/jmsj.82.1599

Webster, P.J., Magaña, V.O. and Palmer, T.N. et al., 1998. Monsoons: Processes, predictability, and the prospects for prediction. Journal of Geophysical Research: Oceans, 103(C7): 14451-14510. DOI: 10.1029/97JC02719

Wilby, R.L. and Harris, I., 2006. A framework for assessing uncertainties in climate change impacts: Low-flow scenarios for the River Thames, UK. Water Resources Research, 42(2): W02419. DOI: 10.1029/2005WR004065

Yatagai, A., Kamiguchi, K. and Arakawa, O. et al., 2012. APHRODITE: Constructing a Long-Term Daily Gridded Precipitation Dataset for Asia Based on a Dense Network of Rain Gauges. Bulletin of the American Meteorological Society, 93(9): 1401-1415. doi:10.1175/BAMS-D-11-00122.1

Yira, Y., Diekkruger, B., Steup, G. and Bossa, A.Y., 2017. Impact of climate change on hydrological conditions in a tropical West African catchment using an ensemble of climate simulations. HYDROLOGY AND EARTH SYSTEM SCIENCES, 21(4): 2143-2161. DOI: 10.5194/hess-21-2143-2017

You, Q., Min, J. and Fraedrich, K. et al., 2014. Projected trends in mean, maximum, and minimum surface temperature in China from simulations. Global and Planetary Change, 112: 53-63. DOI: 10.1016/j.gloplacha.2013.11.006

Yu, Z., Pollard, D. and Cheng, L., 2006. On continental-scale hydrologic simulations with a coupled hydrologic model.

Journal of Hydrology, 331(1–2): 110-124. doi:10.1016/j.jhydrol.2006.05.021

Zhou, T. and Yu, R., 2006. Twentieth-Century Surface Air Temperature over China and the Globe Simulated by Coupled Climate Models. Journal of Climate, 19(22): 5843-5858. DOI: 10.1175/JCLI3952.1

Zou, L., Qian, Y., Zhou, T. and Yang, B., 2014. Parameter Tuning and Calibration of RegCM3 with MIT – Emanuel Cumulus Parameterization Scheme over CORDEX East Asia Domain. Journal of Climate, 27(20): 7687-7701. DOI: 10.1175/JCLI-D-14-00229.1

Hydrol. Earth Syst. Sci. Discuss., https://doi.org/10.5194/hess-2017-407
Manuscript under review for journal Hydrol. Earth Syst. Sci.
Discussion started: 11 September 2017

Hydrology and Earth System Sciences
Open Access
Discussions

Table Captions

Table 1. RCMs used in this study

Table 2. The future changes in average temperature (T; ℃) and precipitation (P; %) for the five subregions (as shown in Figure 1). The ensemble averages for each statistic are given in the second line. The projections by the forcing GCM are given in the last line.

Hydrol. Earth Syst. Sci. Discuss., https://doi.org/10.5194/hess-2017-407
Manuscript under review for journal Hydrol. Earth Syst. Sci.
Discussion started: 11 September 2017

Hydrology and Earth System Sciences
Discussions

Table 1. RCMs used in this study[a] (Park *et al.*, 2016)

	HadGEM3-RA	RegCM4	MM5	WRF	RSM
Resolution	0.44 °	50km	50km	50km	50km
Dynamic process	Non-hydrostatic	Hydrostatic	Non-hydrostatic	Non-hydrostatic	Hydrostatic
Convective scheme	Revised mass flux scheme	MIT-Emanuel	Kain-Fritch II	Kain-Fritch II	Simplified Arakawa-Schubert
Land surface parameterization	MOSES2	CLM3	CLM3	NOAH	NOAH
Planetary boundary layer	MOSES2 non-local	Holtslag	YSU	YSU	YSU
Spectral nudging	No	Yes	Yes	Yes	Yes
Center of research	MOHC	ICTP	NCAR	NCAR	YSU
References	Davies et al. (2005)	Giorgi et al. (2012)	Cha and Lee (2009)	Skamarock et al.(2005)	Hong et al. (2013)

[a]MOSES= Met Office Surface Exchange Scheme, CLM= Community Land Model, NOAH=Noah Land Surface Model, YSU= Yonsei University scheme, MOHC= The Met Office Hadley Centre, ICTP= The International Centre for Theoretical Physics, NCAR= National Center for Atmospheric Research

5

Table 2. The future changes in average temperature (T; ℃) and precipitation (P; %) for the five subregions (as shown in Figure 1). The ensemble averages for each statistic are given in the second line. The projections by the forcing GCM are given in the last line.

		WRF	MM5	HadGEM3-RA	RegCM	RSM	Ensemble	HadGEM2-AO
Northeast China	T(℃)	0.2	2.7	1.4	1.4	1.1	1.3	0.8
	P(%)	-21.7	8.2	13.0	4.4	7.1	1.5	-0.4
North China	T(℃)	0.3	1.7	1.1	1.0	1.0	1.0	0.8
	P(%)	-1.5	15.1	3.1	10.2	3.3	6.1	4.9
South China	T(℃)	0.5	1.5	1.0	0.8	0.8	0.9	0.7
	P(%)	-14.6	-1.6	4.8	4.9	1.3	-1.5	2.3
Northwest China	T(℃)	1.3	0.8	1.5	1.3	1.1	1.2	1.2
	P(%)	-27.0	19.4	2.2	4.7	8.9	3.6	7.2
Tibetan Plateau	T(℃)	0.9	1.4	1.2	1.3	1.6	1.3	1.4
	P(%)	-31.6	-17.8	2.4	6.4	7.4	-7.8	2.1

Figure Captions

Figure 1. The simulation domain of CORDEX-EA and the topography of the regional climate models (m). The boxes illustrate the five selected subregions over China: Northeast China (NE), North China (NC), South China (SC), Northwest China (NW), and Tibetan Plateau (TP).

Figure 2. Spatial distributions of annual average temperature (℃) of CRU (a), multi-model ensemble (b), and temperature biases (℃) of the driving GCM HadGEM2-AO (c), multi-RCM ensemble (d) and five RCMs (e-i) during 1980-2005.

Figure 3. Spatial distributions of annual average precipitation (mm/year) of CRU (a), APHRO (b), multi-model ensemble (c), and precipitation biases (%) of the driving GCM HadGEM2-AO (d), multi-RCM ensemble (e) and five RCMs (f-j) during 1980-2005.

Figure 4. Taylor diagram to compare the skill of the models in representing the summer precipitation over the five regions of China, using the CRU (for temperature) and APHRO (for precipitation) data as the OBS. The azimuthal axis shows the pattern spatial correlation. The redial distance from the origin represents the spatial variability, while the distance from the OBS point is the centered RMSE difference between the simulated and observed.

Figure 5. The temporal evolution of the annual mean temperature (left two panels) and precipitation (right two panels) in RCM simulations and observation over five subregions during the 1989-2007 (Eval) and 1980-2005 (Hist) periods. The correlation coefficient between RCMs ensemble and the observation are shown at the top right of each panel.

Figure 6. Observed and simulated multiyear average of monthly temperature and precipitation over the five subregions during the 1989-2007 (Eval) and 1980-2005 (Hist) periods.

Figure 7. Projected future changes (RCP4.5-Baseline) in surface air temperature for each of the five RCM.

Figure 8. Projected future changes ((RCP4.5-Baseline)/Baseline×100%) in precipitation for each of the five RCM.

Figure 9. Projected future changes in monthly mean temperature and precipitation for each of the five RCM under RCP4.5 scenario.

Figure 10. The fraction of total variance in future temperature (left panel) and precipitation (right panel) projections explained by intermodel variability (gray) and internal variability (white) over the five subregions.

Hydrol. Earth Syst. Sci. Discuss., https://doi.org/10.5194/hess-2017-407
Manuscript under review for journal Hydrol. Earth Syst. Sci.
Discussion started: 11 September 2017

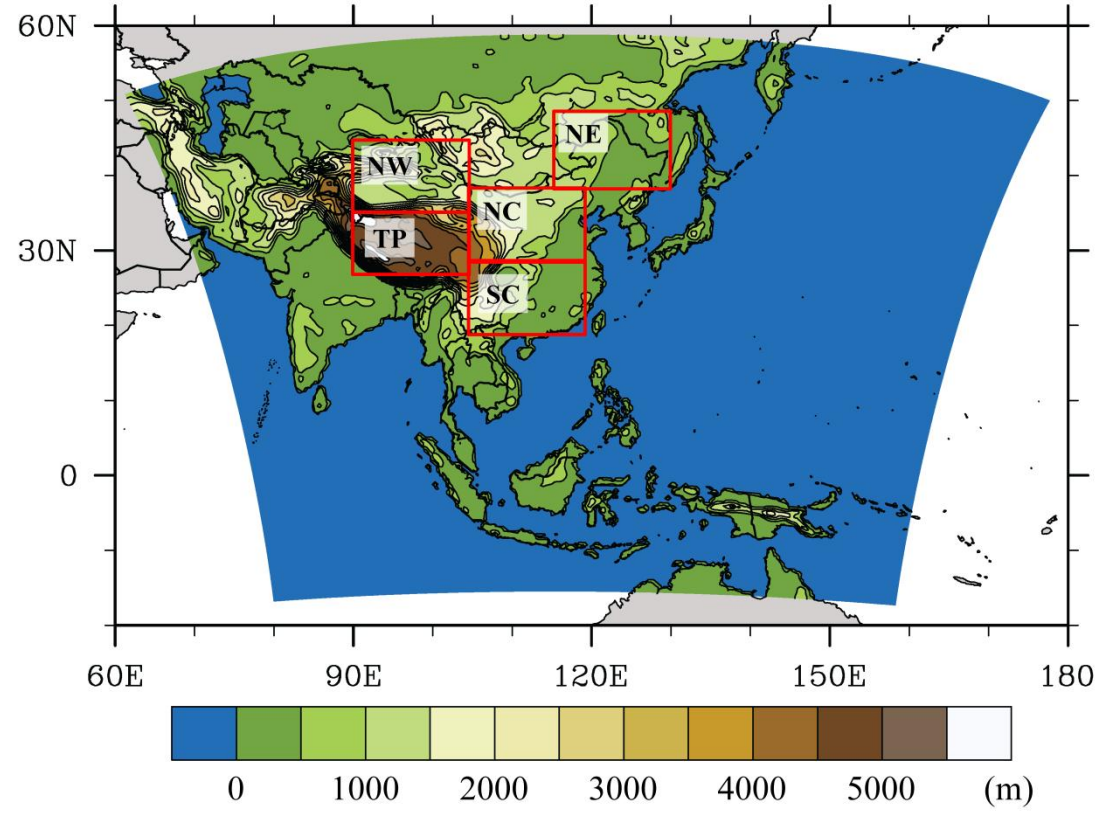

Figure 1. The simulation domain of CORDEX-EA and the topography of the regional climate models (m). The boxes illustrate the five selected subregions over China: Northeast China (NE), North China (NC), South China (SC), Northwest China (NW), and Tibetan Plateau (TP).

Hydrol. Earth Syst. Sci. Discuss., https://doi.org/10.5194/hess-2017-407
Manuscript under review for journal Hydrol. Earth Syst. Sci.
Discussion started: 11 September 2017

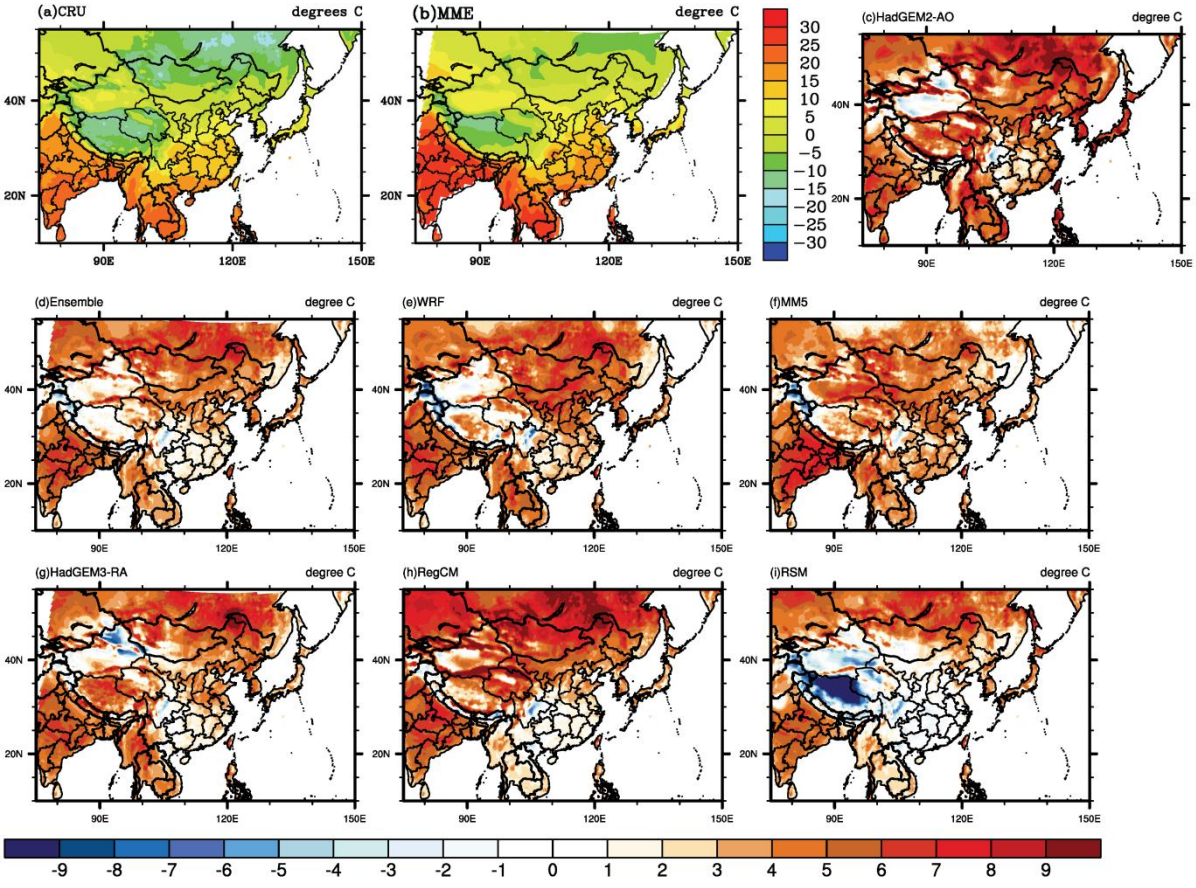

Figure 2. Spatial distributions of annual average temperature (℃) of CRU (a), multi-model ensemble (b), and temperature biases (℃) of the driving GCM HadGEM2-AO (c), multi-RCM ensemble (d) and five RCMs (e-i) during 1980-2005.

Hydrol. Earth Syst. Sci. Discuss., https://doi.org/10.5194/hess-2017-407
Manuscript under review for journal Hydrol. Earth Syst. Sci.
Discussion started: 11 September 2017

Hydrology and Earth System Sciences
Discussions

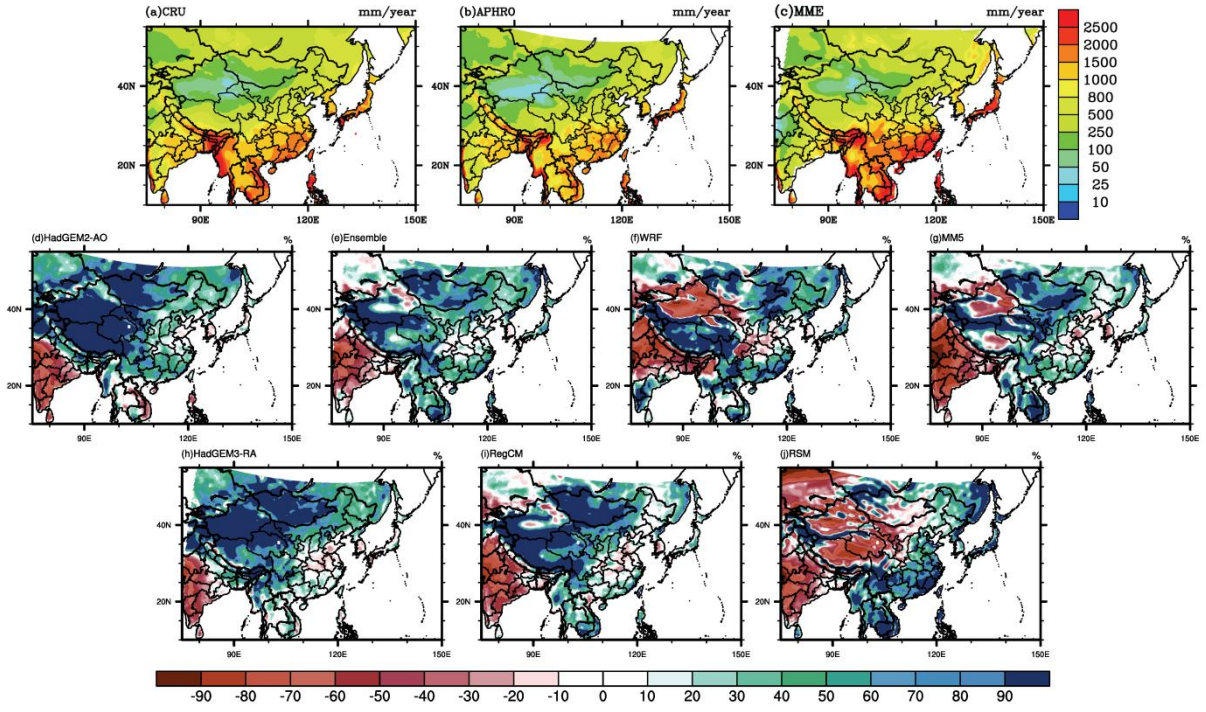

Figure 3. Spatial distributions of annual average precipitation (mm/year) of CRU (a), APHRO (b), multi-model ensemble (c), and precipitation biases (%) of the driving GCM HadGEM2-AO (d), multi-RCM ensemble (e) and five RCMs (f-j) during 1980-2005.

Hydrol. Earth Syst. Sci. Discuss., https://doi.org/10.5194/hess-2017-407
Manuscript under review for journal Hydrol. Earth Syst. Sci.
Discussion started: 11 September 2017

Hydrology and Earth System Sciences
Discussions

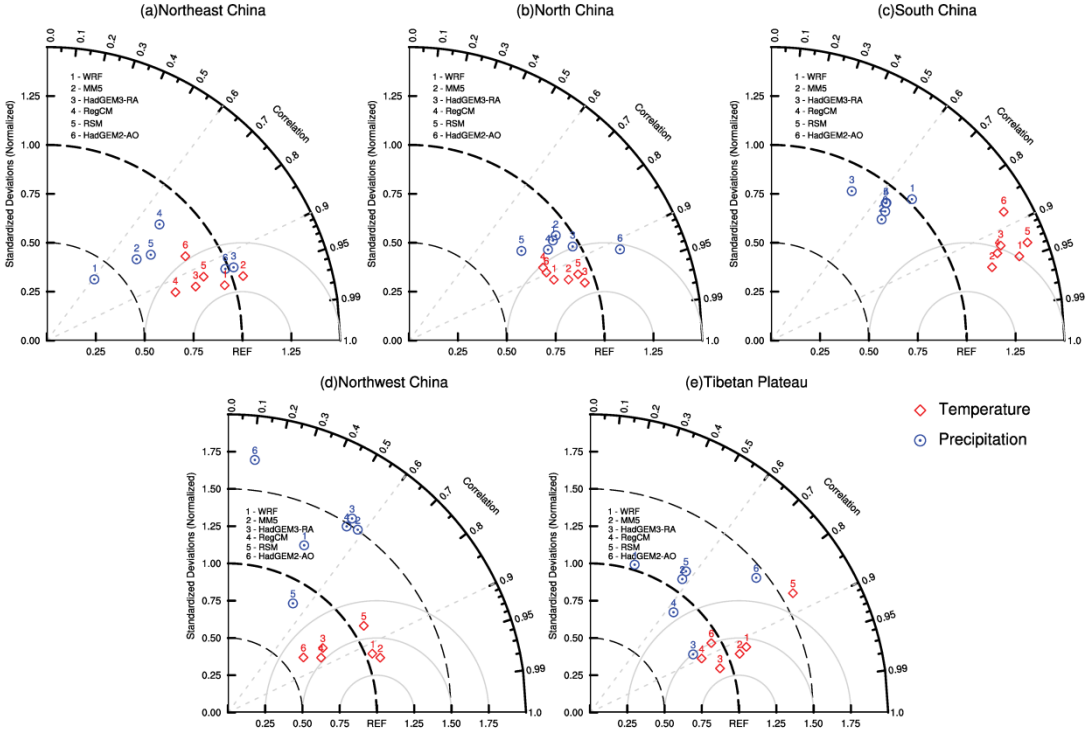

Figure 4. Taylor diagram to compare the skill of the models in representing the summer precipitation over the five regions of China, using the CRU (for temperature) and APHRO (for precipitation) data as the OBS. The azimuthal axis shows the pattern spatial correlation. The redial distance from the origin represents the spatial variability, while the distance from the OBS point is the centered RMSE difference between the simulated and observed.

Hydrol. Earth Syst. Sci. Discuss., https://doi.org/10.5194/hess-2017-407
Manuscript under review for journal Hydrol. Earth Syst. Sci.
Discussion started: 11 September 2017

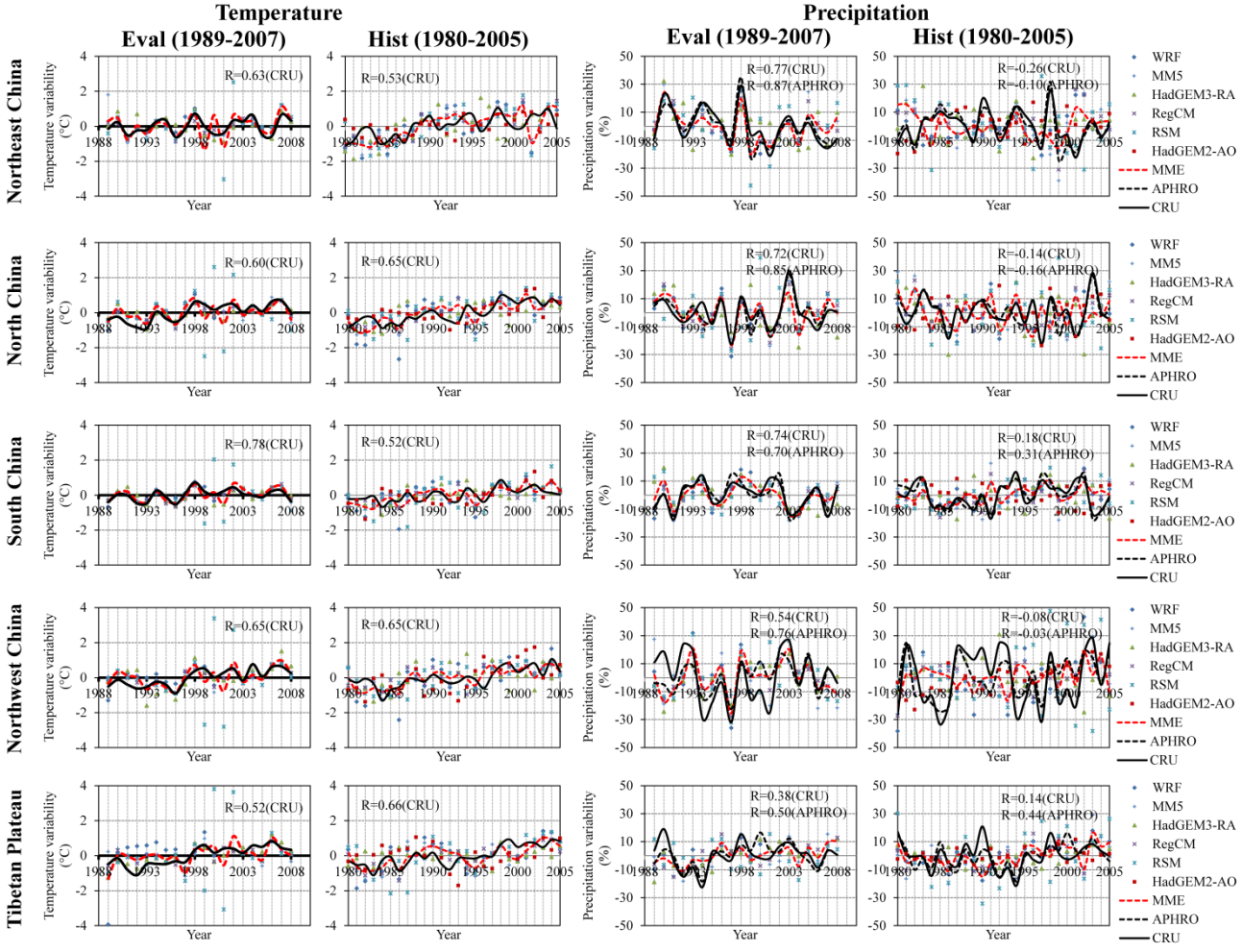

Figure 5. The temporal evolution of the annual mean temperature (left two panels) and precipitation (right two panels) in RCM simulations and observation over five subregions during the 1989-2007 (Eval) and 1980-2005 (Hist) periods. The correlation coefficient between RCMs ensemble and the observation are shown at the top right of each panel.

Hydrol. Earth Syst. Sci. Discuss., https://doi.org/10.5194/hess-2017-407
Manuscript under review for journal Hydrol. Earth Syst. Sci.
Discussion started: 11 September 2017

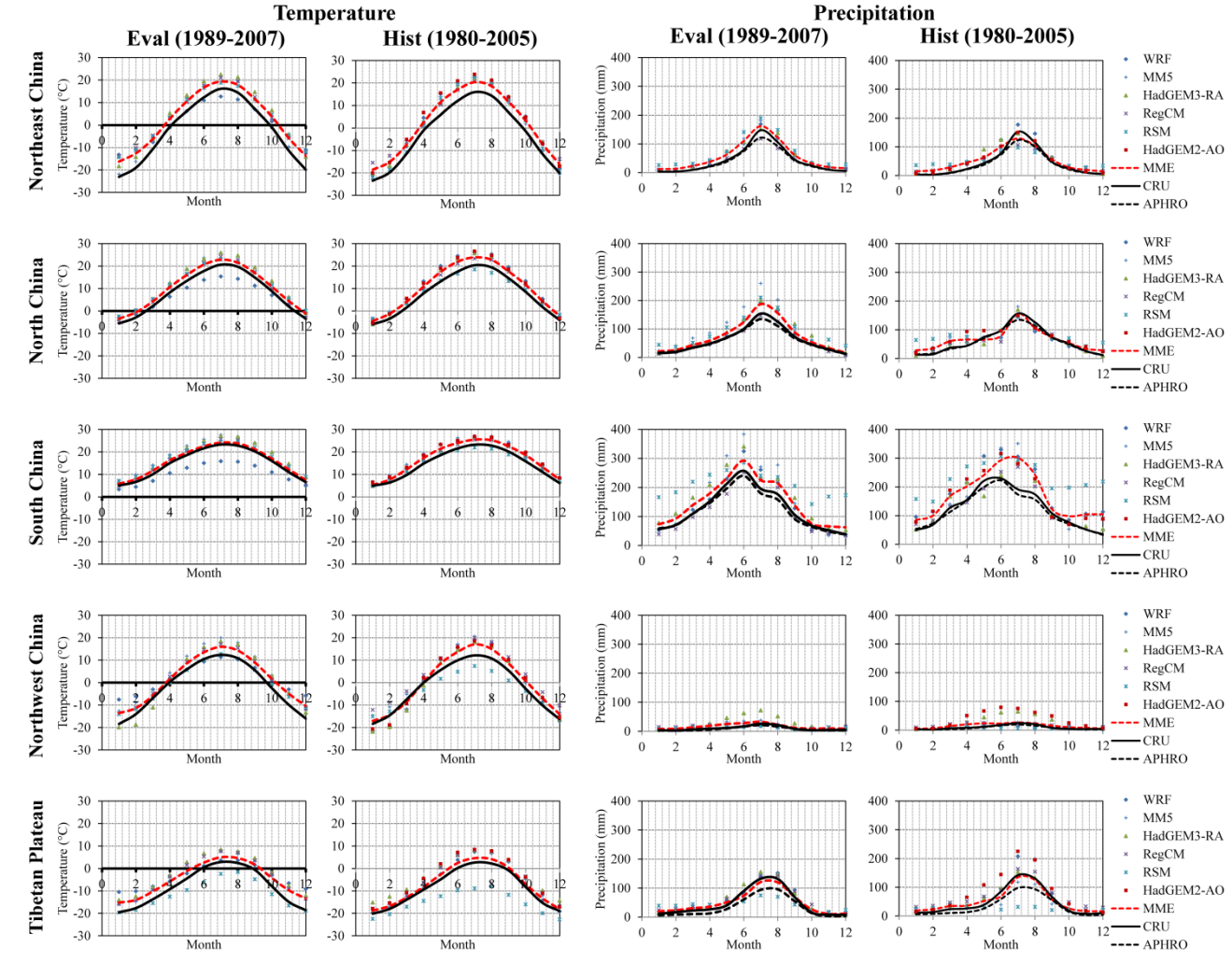

Figure 6. Observed and simulated multiyear average of monthly temperature and precipitation over the five subregions during the 1989-2007 (Eval) and 1980-2005 (Hist) periods.

Hydrol. Earth Syst. Sci. Discuss., https://doi.org/10.5194/hess-2017-407
Manuscript under review for journal Hydrol. Earth Syst. Sci.
Discussion started: 11 September 2017

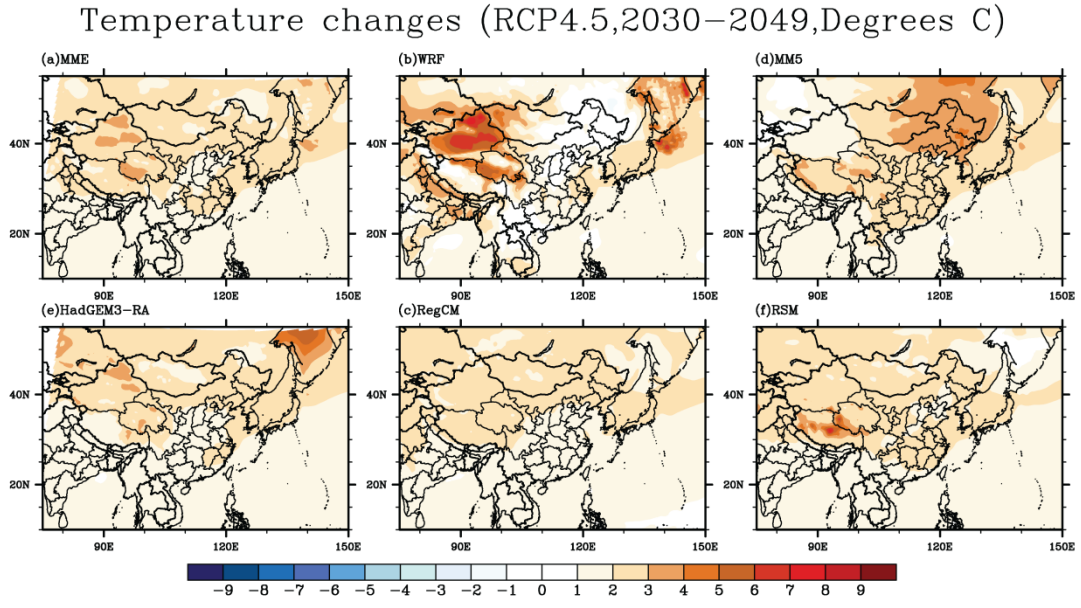

Figure 7. Projected future changes (RCP4.5-Baseline) in surface air temperature for each of the five RCM.

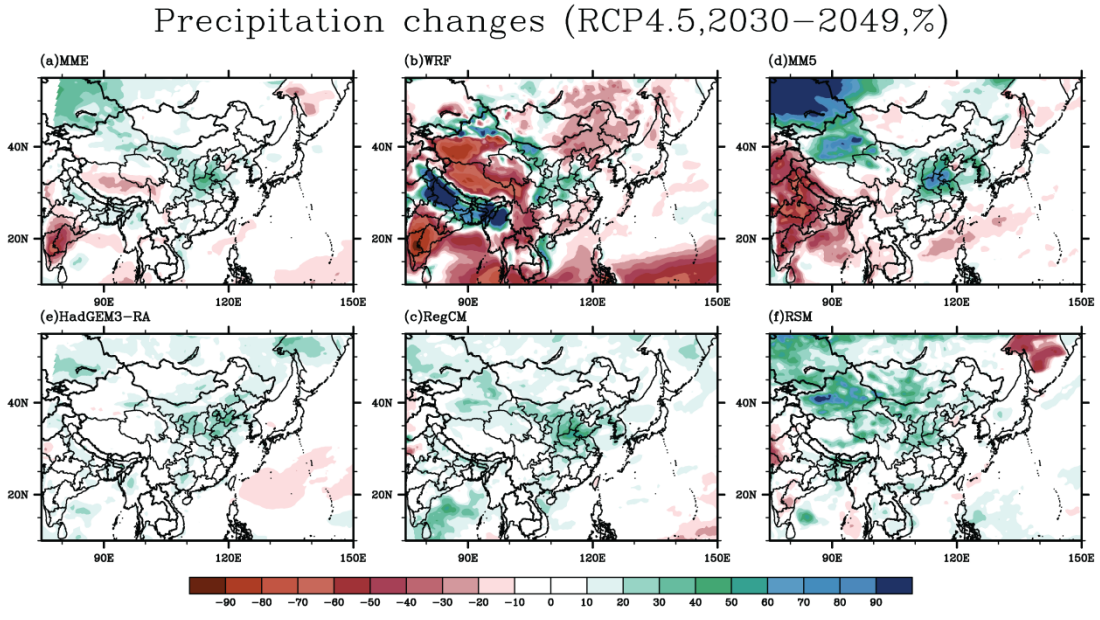

Figure 8. Projected future changes ((RCP4.5-Baseline)/Baseline×100%) in precipitation for each of the five RCM.

Hydrol. Earth Syst. Sci. Discuss., https://doi.org/10.5194/hess-2017-407
Manuscript under review for journal Hydrol. Earth Syst. Sci.
Discussion started: 11 September 2017

Hydrology and Earth System Sciences
Discussions

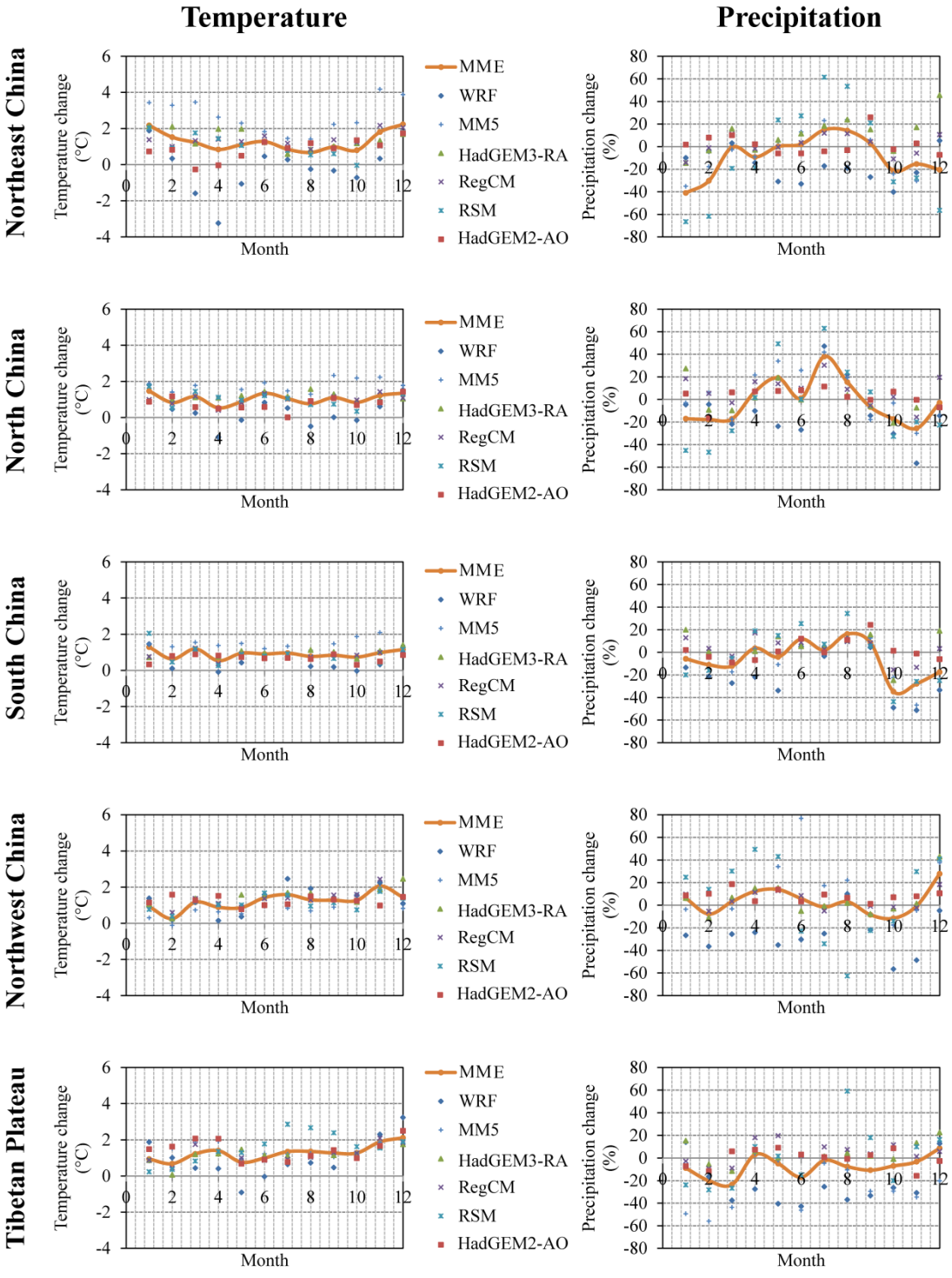

Figure 9. Projected future changes in monthly mean temperature and precipitation for each of the five RCM under RCP4.5 scenario.

Hydrol. Earth Syst. Sci. Discuss., https://doi.org/10.5194/hess-2017-407
Manuscript under review for journal Hydrol. Earth Syst. Sci.
Discussion started: 11 September 2017

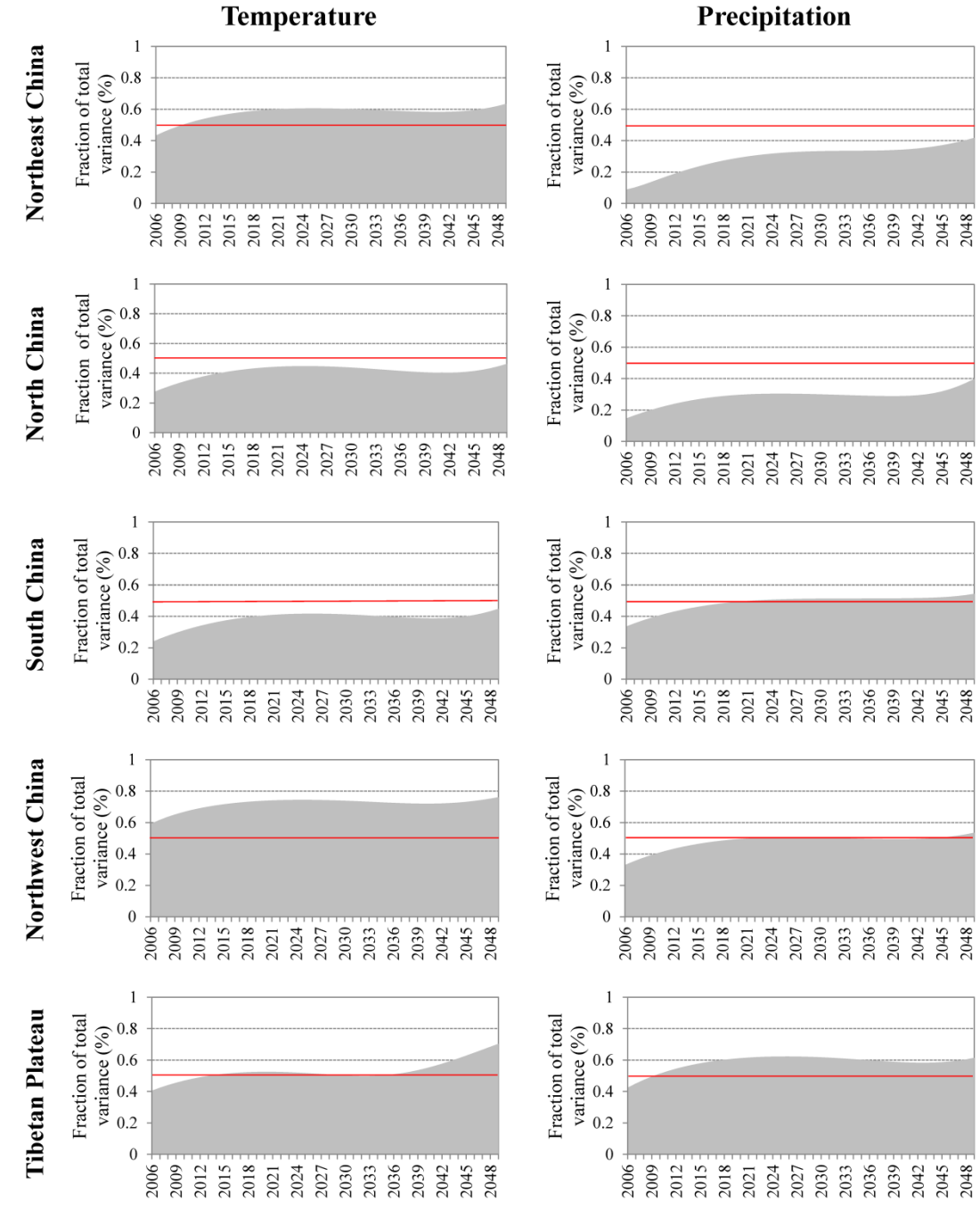

Figure 10. The fraction of total variance in future temperature (left panel) and precipitation (right panel) projections explained by intermodel variability (gray) and internal variability (white) over the five subregions.